NIH Public Access
Author Manuscript
Am J Physiol Cell Physiol. Author manuscript; available in PMC 2014 June 05.

Published in final edited form as:
Am J Physiol Cell Physiol. 2008 March ; 294(3): C662–C674. doi:10.1152/ajpcell.00623.2006.

DIRECT INTERACTION BETWEEN RAB3D AND THE POLYMERIC IMMUNOGLOBULIN RECEPTOR AND TRAFFICKING THROUGH REGULATED SECRETORY VESICLES IN LACRIMAL GLAND ACINAR CELLS

Eunbyul Evans[*], **Wenzheng Zhang**[*], **Galina Jerdeva**, **Chiao-Yu Chen**, **Xuequn Chen**[^], **Sarah F. Hamm-Alvarez**, and **Curtis T. Okamoto**[#]
Department of Pharmacology and Pharmaceutical Sciences, University of Southern California, Los Angeles, CA 90089-9121

[^] Department of Molecular and Integrative Physiology, University of Michigan Medical School, Ann Arbor, MI 48109-0622

Abstract

The lacrimal gland is responsible for tear production, and a major protein found in tears is secretory component (SC), the proteolytically cleaved fragment of the extracellular domain of the polymeric immunoglobulin receptor (pIgR), the receptor mediating the basal-to-apical transcytosis of polymeric immunoglobulins across epithelial cells. Immunofluorescent labeling of rabbit lacrimal gland acinar cells (LGAC) revealed that the small GTPase rab3D, a regulated secretory vesicle marker, and the pIgR are colocalized in subapical membrane vesicles. In addition, the secretion of SC from primary cultures of LGAC was stimulated by the cholinergic agonist carbachol (CCH), and its release rate was very similar to that of other regulated secretory proteins in LGAC. In pull-down assays from resting LGAC, recombinant wild-type rab3D (rab3DWT) or the GDP-locked mutant rab3DT36N both pull down pIgR, but the GTP-locked mutant rab3DQ81L does not. When the pull-down assays are performed in the presence of GTPγS, GTP, or GDPβS, binding of rab3DWT to pIgR is inhibited. In blot overlays, recombinant rab3DWT bound to immunoprecipitated pIgR, suggesting that rab3D and pIgR may interact directly. Adenovirus-mediated overexpression of mutant rab3DT36N in LGAC inhibited CCH-stimulated SC release, and, in CCH-stimulated LGAC, pull-down of pIgR with rab3DWT and co-localization of pIgR with endogenous rab3D were decreased relative to resting cells, suggesting that the pIgR-rab3D interaction may be modulated by secretagogues. These data suggest that the novel localization of pIgR to the regulated secretory pathway of LGAC and its secretion therefrom may be effected by its novel interaction with rab3D.

Keywords

polymeric immunoglobulin receptor; secretory component; rab3D; acinar cells; regulated secretory vesicle; transcytosis; guanine nucleotide exchange factor

[#]Corresponding author: Curtis T. Okamoto, Ph.D. Department of Pharmacology and Pharmaceutical Sciences University of Southern California 1985 Zonal Avenue Los Angeles, CA 90089-9121 Tel: 323-442-3939 Fax: 323-442-1390 cokamoto@usc.edu.
[*]contributed equally to the work, listed alphabetically

NIH-PA Author Manuscript
NIH-PA Author Manuscript
NIH-PA Author Manuscript

NIH-PA Author Manuscript

NIH-PA Author Manuscript

NIH-PA Author Manuscript

INTRODUCTION

The pIgR is expressed in a wide variety of secretory epithelial cells, including those lining the salivary, lacrimal, respiratory, gastrointestinal, hepatic, mammary, and urogenital tracts (36,62). It is a single transmembrane-domain receptor, with a large ligand-binding extracellular domain comprised of 5 immunoglobulin-like domains and a cytoplasmic tail of 103 amino acids. After synthesis in the endoplasmic reticulum and exit from the Golgi, the pIgR is delivered from the trans-Golgi network to the basolateral surface where it binds its ligands, dimeric IgA (dIgA) or pentameric IgM, which represent the primary defense against pathogens at mucosal surfaces (13,14,38,52). With or without its ligand bound at the basolateral surface, pIgR is then endocytosed and transported through a series of endosomal compartments across the cell to the apical surface in the process termed transcytosis (3,7,56). At the apical surface, the extracellular domain of the pIgR that is bound to dIgA is proteolytically cleaved, and secretory IgA (sIgA) is released into the mucosal secretions. If the receptor does not bind to dIgA at the basolateral membrane, this cleaved extracellular domain of the receptor generated apically is known as secretory component (SC).

Tear fluid is relatively rich in sIgA and SC, and the SC concentration in rat tear fluid is 10 times higher than its concentration in saliva (22). The lacrimal gland is the primary source of the aqueous portion of tear film that contains water, electrolytes, and proteins, necessary for the health and maintenance of the ocular surface (25). Proteins in lacrimal gland fluid are secreted predominantly by the acinar cells. We and others have previously reported the presence of the pIgR and SC in LGAC from rabbit (28,47), rat (57,58), and humans (1). LGAC may therefore represent a good, physiologically relevant, organ-based model system to characterize the mechanism of regulation of pIgR trafficking and SC secretion. Thus far, the pIgR-transfected Madin-Darby canine kidney (MDCK) cell line has served as the predominant cellular model for the characterization of the molecular mechanisms that regulate the transcytosis of the pIgR (52).

Key regulators of vesicular traffic are the rab proteins, members of the ras superfamily of small molecular weight guanosine triphosphatases (GTPases) (19,21,45,53,67,77). Rab proteins are known to regulate cargo selection into nascent vesicles, vesicle budding and motility, and tethering, docking, and fusion of vesicles to target organelles. More than 60 Rab proteins have been identified and each is associated with a specific membrane compartment. Four highly homologous rab3 isoforms (rab3A, rab3B, rab3C, rab3D) are expressed in cells with regulated secretory pathways, and these isoforms have been shown to have both positive and negative regulatory functions in a number of steps in regulated secretion (18,54). Of interest here, rab3D is predominantly localized to secretory vesicles of various exocrine secretory cells, such as the acinar cells of the pancreas (41,63), parotid (41,48) and lacrimal glands (16,41,54,73), and chief cells of the stomach (49,59). However, it has also been found in other cell types, usually associated with secretory function, such as neuroendocrine cells (5), osteoclasts (43), endothelial cells (30), alveolar type II cells (68), adipocytes (6), and mast cells (51,61), and it has been localized to the Golgi apparatus in enterocytes and in acinar cells of Brunner’s glands (64).

NIH-PA Author Manuscript

NIH-PA Author Manuscript

NIH-PA Author Manuscript

Functionally, rab3D has been shown to regulate amylase secretion by pancreatic acinar cells. Overexpression of wild-type rab3D in transgenic mice stimulates amylase release (42), and expression of a dominant-negative rab3D in isolated acini inhibits amylase release (12). On the other hand, wild-type rab3D appears to block pepsinogen release from gastric chief cells (40). In addition, in rab3D knock-out mice, functional changes in secretion from exocrine cells were not detected, but these mice had two-fold larger secretory granules in pancreatic and parotid acinar cells, compared to those in wild-type cells (50), suggesting that rab3D may play a role in secretory granule biogenesis. Thus, the role of rab3D in regulating secretion from exocrine cells is still not well defined. The lacrimal gland, with concentrations of rab3D twice that of rab3A in the brain, where rab3A is the most abundant rab (54), may represent a good model system to characterize the role of rab3D in exocrine secretion.

A number of rab proteins have been implicated as possible transcytotic regulators (10,26,29,66,72). Many of these rabs are co-localized with the pIgR and dIgA and regulate their trafficking through particular membrane compartments, such as the apical endosomal compartment. With respect to rab3 isoforms, in pIgR-transfected MDCK cells, endogenous and heterologously expressed rab3B have been shown to interact directly with the pIgR and regulate the transcytosis of pIgR in a GTP-dependent fashion (66). In addition, rab3B binding to pIgR is inhibited when dIgA is added to these transfected MDCK cells, suggesting that the rab3B-pIgR interaction can be regulated by ligand binding and signaling pathways. In rat hepatocytes, rab3D co-purifies with the pIgR in vesicles that are putative transcytotic vesicles (32,33). Thus, depending upon cell type, the rab3 GTPases may also regulate transcytosis, and due to the relatively high expression of both rab3D and pIgR in lacrimal gland, these cells may also represent a good model system to characterize the role of rab3D in the trafficking of pIgR, a marker of the transcytotic pathway.

In work reported here, evidence is presented to support the novel finding that the pIgR is a cargo protein of the regulated secretory pathway in rabbit LGAC and that its trafficking to, or secretion from, this pathway may be regulated by a direct interaction between pIgR and rab3D. The pIgR is localized by immunofluorescence to rab3D-positive vesicles, and pIgR binds to rab3D in pull-down assays and blot overlays. In addition, the interaction of pIgR and rab3D is regulated by CCH stimulation of LGAC and by the GTP-binding state of rab3D, suggesting that the interaction between pIgR and rab3D may be physiologically regulated. Rab3D-dependent trafficking of pIgR into the regulated secretory pathway may occur directly from the TGN or indirectly, via the transcytotic pathway.

MATERIALS AND METHODS

Reagents

CCH, GTPγS, GTP, GDPβS, His-Select Nickel Affinity gel, donkey anti-sheep secondary antibody conjugated to FITC, rhodamine phalloidin, and other chemical reagents were obtained from Sigma-Aldrich (St. Louis, MO). Ni^{2+}-nitriloacetate (Ni-NTA) beads were purchased from Qiagen (Valencia, CA). Protein G-Sepharose was from Pharmacia LKB Biotechnologies Inc. (Alameda, CA). PCR kit and Taq PCRx DNA Polymerase (recombinant) were purchased from Invitrogen (Carlsbad, CA). Total RNA Purification Kit

NIH-PA Author Manuscript

NIH-PA Author Manuscript

NIH-PA Author Manuscript

for cells and tissues was from Gentra Systems (Valencia, CA). High Capacity cDNA Reverse Transcription Kits were obtained from Applied Biosystems (Foster City, CA). Sheep anti-rabbit SC polyclonal antiserum was generated by a commercial vendor (Capralogics, Hardwick, MA) against SC purified from rabbit bile (Pel-Freeze, Rogers, AR) by preparative gel electrophoresis. The antiserum was of sufficient titer to use diluted for Western blotting, immunoprecipitation, and immunofluorescence.

Plasmids encoding $(His)_6$ epitope-tagged forms of wild-type rab3D (rab3DWT), the constitutively active mutant Q81L (rab3DQ81L), and the dominant-negative T36N (rab3DT36N) mutant were gifts from Dr. John A Williams (University of Michigan, Ann Arbor, MI). They were expressed in Escherichia coli (E. coli) and purified on Ni-NTA beads. Anti-rab3D polyclonal antibodies were generated in rabbits against recombinant $(His)_6$ epitope-tagged wild-type rab3D expressed in E. coli and purified by chromatography over protein A/G agarose (Antibodies Inc., Davis, CA). ProLong antifade mounting kit, goat anti-rabbit secondary antibody conjugated to Alexa Fluor-568 and Alexa Fluor-647-phalloidin were from Molecular Probes (Eugene, OR). Goat anti-rabbit IRDye800- and donkey anti-sheep IRDye700-conjugated secondary antibodies were purchased from Rockland (Gilbertsville, PA). Cell culture reagents were from Invitrogen, Inc. (Carlsbad, CA).

Acinar cell isolation and primary culture

Isolation of lacrimal acini from female New Zealand white rabbits (1.8-2.2 kg) obtained from Irish Farms (Norco, CA) was in accordance with the Guiding Principles for Use of Animals in Research and approval from the institution's IACUC. Lacrimal acini were isolated as described (15) and cultured for 2-3 days. Cells prepared in this way aggregate into acinus-like structures while individual cells within these structures display distinct apical and basolateral domains and maintain a robust secretory response (15,16,73). CCH was used at 100 μM to stimulate LGAC.

Isolation of mouse lacrimal glands and olfactory bulbs

Isolation of tissues from Rab3D knockout mice (a generous gift from Dr. Reinhard Jahn, Max Planck Institute for Biophysical Chemistry, Germany) and C57BL/6 mice (Harland, Indianapolis, IN) was in accordance with the Guiding Principles for Use of Animals in Research and approval from the institution's IACUC. The lacrimal gland and olfactory bulb were removed from euthanized C57BL/6 mice and prepared for RT-PCR. Some fragments of the lacrimal gland from C57BL/6 and Rab3D knockout mice were fixed in 4% paraformaldehyde/4% sucrose in Dulbecco's phosphate buffered saline (DPBS) at room temperature for 3–4 hr and then transferred to 30% sucrose in DPBS at 4 °C overnight. The next morning the fragments were dried, immersed in optimum cutting temperature (OCT) solution (Sakura Finetek USA, Torrance, CA), rapidly frozen with liquid nitrogen and cryo-sectioned at 5 μm with a Mikrom cryostat. Cryosections placed on glass coverslips were processed for confocal fluorescence microscopy

NIH-PA Author Manuscript

NIH-PA Author Manuscript

NIH-PA Author Manuscript

Confocal fluorescence microscopy

Reconstituted rabbit lacrimal acini cultured on Matrigel-coated coverslips were fixed and processed as described (15,16,73). Acini were incubated with appropriate primary and fluorophore-conjugated secondary antibodies or Alexa Fluor-647-phalloidin or FITC-phalloidin.

Cryosections of mouse lacrimal glands placed on glass coverslips were sequentially incubated with NH_4Cl, 0.1% Triton X-100, and 1% SDS (each in DPBS), with washes in DPBS between each incubation. Samples were blocked with 1% bovine serum albumin in DPBS and incubated with appropriate primary and fluorophore-conjugated secondary antibodies and rhodamine phalloidin.

Most confocal images were obtained with a Zeiss LSM 510 Meta NLO imaging system (Germany) equipped with Argon, red and green HeNe lasers mounted on a vibration-free table and attached to an incubation chamber controlling temperature, humidity and CO_2. The ability of this system to acquire fluorescence emission signals resolved within narrow ranges in multitrack mode, and the use of singly labeled control samples ensured the validity of co-localization studies by assessing lack of signal bleed-through. Analysis of the extent of colocalization between rab3D and SC/pIgR was determined using similar to the methods described in (28). With the Enhanced Colocalization tool available with the Zeiss LSM510 software, the thresholding function was used to establish background intensity, then a region of interest was selected around the luminal area that was less than 2.0 μm beneath the apical actin. The channel representing SC/pIgR was used to calculate the colocalization coefficient, c, which was calculated as follows: c = colocalizing pixels/total pixels. The coefficient represents the ratio of the sum of intensities of colocalizing pixels with the overall sum of pixel intensities above threshold. The values range from 0 to 1 with 0 representing no colocalization and 1 representing complete colocalization. Panels of images were compiled in Adobe Photoshop 7.0 (Adobe Systems Inc, Mountain View, CA).

RT-PCR for rab3 proteins

The olfactory bulbs and lacrimal glands collected from C57BL/6 mice were homogenized with Polytron PT-2100 tissue homogenizer (Kinematica, Inc, Newark, NJ) in the lysis buffer provided in the Total RNA Purification Kit for Cells and Tissues was from Gentra Systems. The protocol provided by the company was used to prepare total RNA. RT was carried out using a protocol provided by ABI in the High Capacity cDNA RT Kit. RT was conducted with total RNA at a concentration of 1 μg per 10 μl of reaction at 25°C for 10 minutes, 37°C for 2 hours, 85°C for 5 seconds and 4°C overnight. The PCR reaction was performed with a PCR Kit from Invitrogen. The sequences of the primer pairs used were: rab3A, (5′-ATGAGCGAGTGGTGTCCTCA and 5′-GGAGCAGCAGTGACCACAAT); rab3B, (5′-GGAAAGAGTGGTCCCAACTG and 5′-TAATGGAGAGAAGCGGAGGA); rab3C, (5′-TTGGGATAATGCCCAGGTTA and 5′-GGGACATTAGCAGCCACAGT); and, rab3D, (5′-ACGAACGGGTCGTACCTGCT and 5′-GCCCTGAGCTGAGAGACAGT). PCR conditions were programmed in a GeneAmp PCR System 9700 from ABI in the order of 4 cycles as follows: cycle 1 (1X), 94°C for 5 min; cycle 2 (35X), 94°C for 45 sec, 58°C for 45

NIH-PA Author Manuscript

NIH-PA Author Manuscript

NIH-PA Author Manuscript

sec, 72°C for 1 min; cycle 3 (1X), 72°C for 6 min; and, cycle 4 (1X), 4°C, overnight. These PCR fragments were analyzed by 1.2% agarose gel electrophoresis.

Adenoviral constructs and transduction

Replication-defective adenoviral (Ad) constructs used in these studies include Ad encoding $(His)_6$-tagged wild-type rab3D (rab3DWT) and green fluorescent protein (GFP) separately (Ad-rab3dWT), Ad encoding $(His)_6$-tagged dominant-negative rab3DT36N (rab3DT36N) and GFP separately (Adrab3DT36N), Ad encoding $(His)_6$-tagged constitutively active rab3DQ81L (rab3DQ81L) and GFP separately (Ad-rab3DQ81L), Ad encoding GFP alone (Ad-GFP) (73), and Ad encoding a syncollin-GFP fusion protein (Ad-syncollin-GFP) (a kind gift of Dr. Chris Rhodes, University of Chicago). All the Ad-rab3D constructs were generous gifts from Dr. John A. Williams (University of Michigan, Ann Arbor, MI). Reconstituted rabbit LGAC cultured for 2 days were exposed to the Ad constructs for 1-2 hours at a multiplicity of infection (MOI) of 5, then washed twice with Dulbecco's PBS and incubated in fresh culture medium for 18-20 hours at 37°C and 5% CO_2. On day 3 of culture, transduction efficiency was determined by observing the GFP fluorescence. Lacrimal acinar cultures with at least an ~80% efficiency of cellular transduction, as determined by GFP expression, were used for analysis.

SC secretion analysis

Rabbit lacrimal gland acini seeded on Matrigel-coated 12-well plates were transduced on day 2 with Ad-syncollin-GFP, Ad-rab3DWT, Adrab3DT36N, Ad-rab3DQ81L, or Ad-GFP. On day 3 of culture, untransduced or transduced lacrimal acini were stimulated with CCH (100 μM) and the media was collected at time points up to 30 min. The cell pellets were dissolved in 0.5 N NaOH. Equal volumes of the media were concentrated in YM-10 Microcons (Millipore, Bedford, MA) and resolved by SDS-PAGE. Proteins of interest were detected by Western blotting. Signal intensities were quantitated and normalized to pellet protein for each sample.

Pull-down of rab3D and pIgR

$(His)_6$ epitope-tagged forms of rab3DWT, the constitutively active mutant rab3DQ81L, and the dominant-negative mutant rab3DT36N were expressed in E. coli and purified on Ni-NTA bead columns. 3.6×10^7 resting or CCH-stimulated LGAC, or 5.0×10^7 MDCK cells were solubilized in a buffer containing 1% Triton X-100, 20mM Na-HEPES, pH 7.4, and 50mM KCl, and incubated overnight at 4°C with 40 μg of recombinant wild-type or mutant rab3D. In some cases, the lysate was supplemented with 10 μM nonhydrolyzable GTPγS, 10 μM nonhydrolyzable GDPβS, or 0.5 mM GTP. Rab3D was recovered from the lysates by incubation with His-Select Nickel Affinity Gel beads for 1 hour at room temperature and washed. Rab3D and any interacting proteins were eluted from the beads with SDS-PAGE sample buffer, and analyzed on Western blots.

Immunoprecipitation and overlay

Resting LGAC (7.2×10^7 cells) were solubilized in a buffer containing 2.5% Triton X-100, 100 mM triethanolamine, pH 8.6, 100 mM NaCl, 5 mM EDTA, and 0.02% NaN_3, and pIgR

NIH-PA Author Manuscript

NIH-PA Author Manuscript

NIH-PA Author Manuscript

was immunoprecipitated at 4°C overnight with anti-SC polyclonal antibodies covalently coupled to Protein G-Sepharose (6 μl of packed beads). After washing, the immunoprecipitate was resolved by SDS-PAGE, and transferred to nitrocellulose membrane. The membrane was soaked in a solution containing 50 mM Tris-HCl, pH 7.5, 150mM NaCl, 1mM DTT, 0.3% Tween-20, 3% BSA, 0.05% NaN_3 for 6 - 7 h at room temperature, then incubated with 10 μg recombinant rab3DWT in 10 ml of a solution containing 10 mM Tris-HCl, pH 7.5, 20mM NaCl, 1mM DTT, and 0.5 mM EGTA at 4°C overnight. After washing, the membrane was analyzed on Western blot.

Nitrocellulose membrane stripping

Nitrocellulose membrane was soaked in a buffer containing 100 mM 2-mercaptoethanol, 62.5 mM Tris-HCl, pH 6.8, and 2% SDS at 50°C for 30 min to strip previously bound primary and secondary antibodies. After washing and blocking, the membrane was reprobed with appropriate new primary and secondary antibodies and analyzed on Western blot.

Western blots

Western blots were processed utilizing appropriate primary antibodies and secondary antibodies conjugated to either IRDye-800 or IRDye-700. Blots were quantified using Li-Cor Odyssey Scanning Infrared Fluorescence Imaging System (Lincoln, NE). For display, fluorescent signals were converted digitally to black and white images.

RESULTS

Expression of rab 3 isoforms in mouse lacrimal glands

The expression of mRNA for rab3 isoforms in lacrimal glands was characterized by RT-PCR. Due to the lack of sequence information in the database for rabbit rab3 isoforms, primers specific for each mouse rab3 isoform were used to amplify fragments from mouse lacrimal glands. As shown in Figure 1A, only rab3A and rab3D (lanes 5 and 8, respectively) appear to be expressed in mouse lacrimal glands. On the other hand, rab3A, 3B, 3C, and 3D (lanes 1, 2, 3, and 4, respectively) are all expressed in mouse olfactory bulb.

The specificity of the rab3D antiserum was characterized by immunofluorescent labeling of isolated mouse lacrimal glands from rab3D knock-out (KO) mice and wild-type mice. As shown in Figure 1B, there is little immunoreactivity observed in lacrimal glands from rab3D knock-out mice, compared to that observed in glands from wild-type mice. These data suggest that the antiserum is apparently specific for rab3D and does not cross-react to a significant degree with rab3A in lacrimal glands.

pIgR and rab3D are co-localized in resting LGAC

The intracellular distributions of pIgR/SC and rab3D were analyzed by confocal fluorescence microscopy of primary cultures of reconstituted lacrimal acini. The polyclonal anti-SC antiserum recognizes both full-length pIgR and SC. Analysis of the immunofluorescence associated with pIgR/SC (Figure 2, green), revealed that pIgR/SC immunoreactivity was distributed on the basolateral membrane (BLM), and additional pIgR/SC immunoreactivity was detected in large apparent vesicles or organelles localized

NIH-PA Author Manuscript

NIH-PA Author Manuscript

NIH-PA Author Manuscript

beneath the apical plasma membrane (APM) (Figure 2, arrows) surrounding the luminal regions (Figure 2, asterisk). Rab3D, a regulated secretory vesicle (SV) marker, (Figure 2, red) also was localized to this subapical region in similar structures. In the merged image, there appeared to be significant colocalization of the pIgR/SC and rab3D signals near the apical membrane. Quantitation of the co-localization between the signals from the two proteins revealed that about 40% of the total cellular rab3D pixels were co-localized with those of pIgR/SC (Figure 2, yellow). These results are the first to show the co-localization of pIgR/SC with a marker protein of regulated secretory vesicles, rab3D, and suggest that the pIgR/SC is a cargo protein packaged into regulated SV in LGAC.

Profile of SC release from carbachol-stimulated LGAC

Syncollin is a protein that was originally characterized to be tightly associated with the luminal surface of zymogen granules in pancreatic acinar cells (2). Syncollin-GFP fusion protein has been used to label large protein-enriched secretory vesicles in a variety of cell types (23,24). Previous studies of syncollin-GFP in rabbit lacrimal gland acinar cells show that acini transduced with adenovirus encoding for syncollin-GFP (Ad-syncollin-GFP) expressed syncollin-GFP in large mature secretory vesicles underneath the apical plasma membrane in unstimulated lacrimal acini (27,28). If pIgR/SC is packaged into regulated secretory vesicles, its rate of release should parallel that of other secreted marker proteins in the regulated secretory pathway, such as syncollin-GFP. To analyze the release pattern of the exogenously expressed syncollin-GFP, a mature secretory vesicle marker, media was collected from Ad-syncollin-GFP transduced acini, concentrated, and immunoblotted with an anti-GFP antibody. Analysis of the Western blots, which were quantitated and normalized to total cellular protein, revealed a rapid burst of release of syncollin-GFP within the first 5 min of CCH stimulation (Figure 3A). Between 5 and 15 min of CCH stimulation, the rate of release of syncollin-GFP was slower, and after 15 min, the rate of release increased again. To determine the release pattern of SC and compare it to that of syncollin-GFP, media collected from untransduced lacrimal gland acinar cells was concentrated and immunoblotted with anti-SC antibodies. Analysis of the Western blots of SC release after CCH treatment revealed a release pattern similar to that of syncollin-GFP in the early phase of release (Figure 3B). SC was rapidly released within the first 5 min of CCH stimulation, consistent with SC or pIgR residing in a secretagogue-sensitive pool of mature secretory vesicles.

Recombinant rab3D binds to pIgR in pull-down assays

One possibility that would contribute to the significant co-localization of pIgR/SC and rab3D in LGAC is that rab3D and full-length pIgR may interact to regulate pIgR localization to regulated secretory vesicles or pIgR/SC secretion therefrom. Attempts at co-immunoprecipitation were not successful (data not shown). Thus, pull-down assays with recombinant $(His)_6$-tagged rab3DWT were performed. Different amounts (40 μg or 80 μg) of recombinant rab3D protein were used in pull-down assays with lysates from resting (unstimulated) LGAC. Rab3DWT could successfully pull down pIgR from these lysates, indicating that rab3D can associate with pIgR (Figure 4). In addition, the amount of pIgR pulled down with rab3DWT was proportional to the amount of rab3DWT protein added.

NIH-PA Author Manuscript

NIH-PA Author Manuscript

NIH-PA Author Manuscript

Rab3D-pIgR interaction is sensitive to the GTP-bound state of rab3D

If the interaction between rab3D and pIgR is functionally significant, the state of GTP binding to rab3D should affect its interaction with pIgR. To examine how the GTP binding state of rab3D influenced rab3D-pIgR interaction, the binding of pIgR to rab3DWT or mutated rab3D proteins was tested in pull-down assays. Although background binding of pIgR in these assays was observed, pull-down of pIgR from resting LGAC lysates with either recombinant WT or mutant rab3D proteins showed that pull-down of pIgR by rab3DWT and the putative dominant-negative mutant rab3DT36N was significantly increased (Figure 5A). In fact, rab3DT36N bound 36% ± 19% more pIgR (S.E.M., n=3 independent experiments), compared to pIgR binding to rab3DWT. On the other hand, the constitutively active rab3DQ81L, did not bind to pIgR (Figure 5A), only 4% ± 4% (S.E.M., n=3 independent experiments) of the amount of pIgR bound to rab3DWT. Furthermore, as shown in Figures 5A and 5B, when 10 μM GTPγS or 0.5 mM GTP is added to the lysates used in the pull-down assays with rab3DWT, binding of pIgR is also significantly inhibited, only 9% ± 5% (S.E.M., n=7 independent experiments) and 25% ± 8% (S.E.M., n=9 independent experiments), respectively, of the amount of pIgR bound to rab3DWT. Interestingly, incubation of rab3DWT with GDPβS in the pull-down assay also inhibited pIgR binding (Figure 5C and 5D). These data suggest that the interaction of pIgR with rab3D is sensitive to the GTP-bound state of rab3D. The GTP-bound form of rab3D, whether induced by a mutation or by addition of GTP or GTPγS, appears to be incapable of interacting with pIgR. The interaction of pIgR with rab3D is more complex with the GDP-bound form of rab3D, since the T36N mutation allows the mutated rab3D to bind effectively to pIgR, while the addition of GDPβS to wild-type rab3D inhibits binding of pIgR.

Similar experiments were performed in pIgR-transfected MDCK cells with the same concentration of GTPγS or GTP included in the pull-down assays. Figure 5E demonstrates that binding of rab3D and pIgR can be replicated in pIgR-transfected MDCK cells. In addition, rab3DWT did not bind to pIgR when GTPγS or GTP was added in the pull-down assays. Thus, the binding characteristics of rab3D and pIgR from LGAC can be reproduced with pIgR-transfected MDCK cells, indicating that the interaction of rab3D with pIgR may be independent of the source of pIgR-containing cell lysates.

Direct interaction between rab3D and pIgR

The pull-down assays do not distinguish whether the interaction between rab3D and pIgR is a direct or indirect one. Thus, blot overlay assays (far Western blots) were performed to test whether rab3D and pIgR can interact directly. The pIgR was immunoprecipitated from LGAC, resolved on SDS-PAGE, and transferred to nitrocellulose. The blot was then incubated with recombinant rab3DWT and probed with anti-rab3D antibody to detect where rab3D had bound to the blot. As shown in Figure 6 (left lane), two proteins, one migrating with an Mr of ~120 kDa and the other at ~130 kDa, showed significant binding to rab3D. To confirm whether the lower Mr band was pIgR, the blot was stripped of rab3DWT and was reprobed with anti-SC antibody to detect pIgR. As shown in the right lane in Figure 6, the anti-SC antibodies reacted with the protein migrating at ~120 kDa. Upon comparison of both blots, the 120 kDa protein binding to rab3D and anti-SC immunoreactivity coincided precisely. Immunoprecipitated SC, migrating around ~80 kDa, did not bind to rab3D. These

NIH-PA Author Manuscript

NIH-PA Author Manuscript

NIH-PA Author Manuscript

results are consistent with a direct interaction between rab3D and pIgR, and this interaction appears to be dependent upon the presence of the cytoplasmic and/or membrane spanning domain of pIgR.

Adenovirus-mediated overexpression of mutant rab3DT36N in LGAC inhibits CCH-stimulated SC secretion

If the rab3D-pIgR interaction regulates SC release via direct interaction with each other, overexpression of rab3D or its mutants should have functional effects on pIgR trafficking and SC secretion. In particular, since SC secretion appears to be stimulated by CCH, overexpression of rab3D or its mutants should affect CCH-stimulated SC secretion. Analysis of SC release from lacrimal gland acini transduced with Ad-rab3D constructs (Figure 7, A-C) reveal that in acini overexpressing the mutant rab3DT36N, the release of SC attributed to only CCH stimulation (i.e., the basal rate of SC release is subtracted) is significantly inhibited after 15 min of stimulation compared to that of Ad-GFP transduced acini (Figure 7B). In all other cases, there were no statistically significant differences in SC secretion between the control lacrimal glands and those overexpressing the various rab3D constructs (Figures 7A and 7C), and there were no effects of overexpression of rab3D on basal SC secretion (data not shown). Nonetheless, inhibition of CCH-stimulated SC secretion by rab3DT36N is consistent with a role for rab3D in regulating pIgR trafficking and SC release through the regulated secretory pathway.

The lack of clear-cut functional effects from the overexpression of rab3D, particularly the mutants, suggests that the regulation of SC release by rab3D may be much more complex than acting as a binary switch or that perhaps other isoforms of rab3 (such as rab3A) may be compensating for the compromised function of rab3D.

Acute treatment of cholinergic agonist abolishes rab3D-pIgR binding

We have previously reported that 100 μM CCH stimulated the acute (30 min) release of SC from LGAC (28). CCH may then regulate the interaction of pIgR with rab3D, ultimately to regulate SC release from LGAC. Stimulation of LGAC secretion with 100 μM CCH for 30 min or 60 min prior to lysis, followed by incubation of lysates with recombinant rab3DWT in pull-down assays, resulted in a loss of pIgR binding to rab3DWT from 100% (0 min) to 43% ± 15% (30 min) and 26% ± 13% (60 min) (S.E.M., n=5 independent preparations) (Figures 8A and 8B). Although there is a decrease in pIgR content in acini after stimulation by CCH (Figures 8C and 8D), the magnitude and time course of this decrease differ from those observed in the pull-down assays, suggesting that the overall decrease in pIgR content in the acini appears to be unlikely to account for the decrease in pIgR binding to rab3D in the pull-down assays from CCH-stimulated cells. Thus, the CCH-dependent physiological signaling pathway in LGAC modulates the interaction between rab3D and pIgR. The CCH-dependent loss of interaction between rab3D and pIgR could provide a mechanism for the observed stimulation of SC secretion in lacrimal acinar cells, particularly if the rab3D-pIgR interaction negatively regulates the terminal steps in SC release.

This CCH-dependent loss of binding of pIgR to rab3D is consistent with qualitative confocal microscopic observations on the CCH-dependent changes in co-localization of pIgR and

NIH-PA Author Manuscript

NIH-PA Author Manuscript

NIH-PA Author Manuscript

rab3D in CCH-stimulated LGAC (Figure 9A). Upon 5 minutes of carbachol stimulation, rab3D starts dispersing and the colocalization of rab3D and pIgR slightly decreases in the subapical region (Figure 9B). The decrease in colocalization of rab3D and pIgR is even more significant after 30 min of CCH stimulation (Figure 9B), when most of the rab3D has dispersed from the subapical region.

DISCUSSION

Rab3D is a rab family member most commonly found in cells with regulated secretory pathways, such as pancreatic acinar cells (41,63), salivary parotid acinar cells (41,48), lacrimal acinar cells (16,41,54,73), and gastric chief cells (49,59). In many of these cell types, rab3D has also been localized to zymogen granule membranes, suggesting that it may play a role in regulating zymogen granule biogenesis and/or release. In this study, using immunofluorescence, biochemical approaches, and functional assays, we have provided novel evidence in primary cultures of rabbit lacrimal acinar cells for the localization of the pIgR to mature secretory granules, as defined by rab3D-associated membrane compartments, and for the direct interaction of endogenous pIgR with endogenous rab3D. Moreover, evidence is provided that the interaction is sensitive to the GTP-bound status of rab3D, and, surprisingly, when rab3D is in its GTP-bound form, it cannot interact with the pIgR. Finally, the interaction between rab3D and pIgR may be regulated by physiological signaling pathways stimulated by CCH, an acetylcholine receptor agonist, since stimulation of acinar cells with CCH results in a loss of rab3D-labeled membranes by immunofluorescence and a loss of pIgR binding to rab3D in pull-down assays. These apparent CCH-dependent changes in localization of endogenous rab3D and in its interaction with pIgR are concomitant with stimulation of SC release from lacrimal acinar cells, suggesting that rab3D is involved in either the localization or the retention of pIgR in mature secretory granules or that pIgR is involved in targeting of rab3D to mature secretory granules. Interestingly, the data obtained in the pull-down assays are consistent with pIgR acting as a guanine nucleotide exchange factor (GEF) for rab3D. In cases where the interaction between a small GTPase and its GEF have been characterized, the GEF binds better to the nucleotide-free form of the small GTPase compared to either the GTP or the GDP nucleotide-bound forms. These examples include ras binding to its GEF, Son-of-Sevenless (69), and the yeast rab GTPase ypt1 binding to TRAPP (71), a multiprotein complex that regulates vesicle trafficking from the endoplasmic reticulum to the Golgi apparatus. In addition, the crystal structures of several nucleotide-free small GTPases with their GEFs as a stable binary complex have been determined, such as EF-Tu with EF-Ts, ras with Son-of-Sevenless, and Arf with Geα2 (69). In studies with mutants of rab3A, Rab3AT36N has been shown to bind to GDP but exhibits a very high dissociation rate for GDP, up to 60 times higher than that for wild-type rab3A (8). In addition, this particular mutant does not bind GTP (8), nor does the rab3DT36N mutant (X.C., unpublished data), suggesting that it may spend a significant amount of time in the nucleotide-free state in vitro and in vivo. Finally, Rab3AT36N has a 10-fold higher affinity for the Rab3A GEF, rab3A-guanine nucleotide releasing factor, compared to wild-type rab3A (8).

Thus, if pIgR is a GEF for rab3D, and if the rab3DT36N mutant behaves similarly to the identical mutant of rab3A, then, in the pull-down assays: 1) binding of pIgR to wild-type

NIH-PA Author Manuscript

NIH-PA Author Manuscript

NIH-PA Author Manuscript

rab3D should be inhibited in the presence of either GTP or GDP; and, 2) pIgR would bind better to the T36N mutant compared to nucleotide-free or nucleotide-bound wild-type rab3D. Both of these predicted results are observed here. In addition, in vivo, the observed inhibition of SC secretion by adenoviral-mediated expression of rab3DT36N is consistent with this mutant interacting better with pIgR to form unproductive interactions. These data raise the intriguing possibility that pIgR may act as an exchange factor for rab3D. Such an effector function would have two important functional outcomes: 1) rab3D would be targeted to membranes containing pIgR, such as mature secretory granules and the trans-Golgi network; and, 2) rab3D would be activated by exchanging GDP for GTP at the site of action. Testing whether pIgR is a GEF for rab3D is currently underway. Once in the GTP-bound form, rab3D may then recruit effectors for vesicle translocation, vesicle fusion, or sorting of nascent pIgR to new regulated secretory granules. In other cell types, there is significant evidence to support a role for rab3D GTPases in vesicle docking or fusion (5,11,35,40,54) and/or secretory granule biogenesis (43,64).

Alternatively, in previous studies of the inhibitory effect of the expression of the rab3DT36N mutant on the early phase of amylase secretion by pancreatic acinar cells, it was shown that expression of this mutant reduces the level of GTP-bound endogenous rab3D (12), suggesting that it inhibits GDP/GTP exchange on the endogenous rab3D. Expression of the wild-type or constitutively active rab3DQ81L did not alter the levels of GTP-bound endogenous rab3D and did not affect amylase secretion. Thus, the effects of the expression of these proteins in pancreatic acinar cells may be due to their effects on GDP/GTP exchange on endogenous rab3D, and their similar effects on SC secretion by LGAC may be due to similar mechanisms.

On the other hand, the variable effects of rab3D overexpression in LGAC may reflect functional redundancy of other rab3 isoforms expressed in LGAC. We have detected both rab3D and rab3A by RT-PCR analysis of mouse LGAC mRNA; however, at the protein level, another study could only detect rab3D in lacrimal glands (54). We could not independently determine protein levels of rab3A in rabbit LGAC. Nonetheless, the issue of functional redundancy has been well documented for rab3 isoforms (54), as well as the differing and sometimes opposite effects of overexpression of rab3D and its mutants in regulating secretion from other exocrine cells (11,40,42). Finally, the variable effects of overexpression may also be due to the regulation of more than one step of pIgR trafficking by rab3D along the merocrine secretory pathway.

The findings reported here clearly differ in several fundamental aspects from the study of van IJzendoorn, et al. (66), in which rab3B was shown to bind to pIgR in a manner sensitive to the GTP-bound state of rab3B and also to the binding of the pIgR's ligand, dIgA. In contrast to our results with rab3D, they reported that the GTP-bound form of rab3B interacted with pIgR. This difference may reflect the different functional roles of rab3B and rab3D in cell types in which these rabs and pIgR are expressed. Another difference is that while they could reconstitute rab3B binding to the cytoplasmic domain of pIgR in vitro, in those same experiments, they did not detect an interaction between rab3D and pIgR. Since rab3B does not appear to be expressed in lacrimal acini, we have not independently verified that rab3B binds to pIgR in our system; however, we did verify that recombinant rab3D

NIH-PA Author Manuscript

NIH-PA Author Manuscript

NIH-PA Author Manuscript

could bind to pIgR from transfected MDCK cells in pull-down assays. Thus, we interpret these data to suggest that, since both rab3B and rab3D can bind to pIgR directly, there may be a common motif shared by rab3B and rab3D that mediates binding to pIgR. Indeed, van IJzendoorn, et al., have shown that the membrane-proximal 14 amino acids of the cytoplasmic domain of the pIgR are necessary for rab3B-pIgR interaction; interestingly, this region also contains the basolateral targeting motif of the pIgR (4). Alternatively, we might also speculate that both rab3B and rab3D bind to pIgR, but to different motifs on the cytoplasmic domain of the pIgR, and the nature of these interactions are sensitive to the types of fusion proteins used with the in vitro binding assays. Specifically, the previous study used GST fusions of rab3B and the pIgR cytoplasmic domain, while here the $(His)_6$-tagged versions of rab3D and either solubilized pIgR from cell lysates or immunoprecipitated pIgR were used.

Having acknowledged the differences between these two studies, it is probably more instructive to focus upon their similarities. The first is the identification and characterization of a direct interaction between a rab protein and its putative cargo. There are still only a few other cargo proteins that have been shown to interact with rab proteins directly, such as rab5a with the angiotensin-1 receptor (55), rab11a with the Transient Receptor Potential (TRP) V5 and TRPV6 Ca^{2+} channels (65), and rab21 with α-integrin (44).

The second similarity between the van IJzendoorn study and ours is that the interaction between the rab3 isoform and pIgR is sensitive to the GTP-binding state of the rab3 isoform, suggesting that both interactions are functional ones. Third, the interaction between the rab3 isoform and pIgR is also sensitive to physiological stimuli. In the case of rab3B, it is dIgA, and, with rab3D in lacrimal acinar cells, it is CCH. In both cases, these stimuli either prevent binding or stimulate the dissociation of the rab3 isoform and pIgR. Interestingly, both dIgA and CCH stimulate the elevation of intracellular Ca^{2+} in their respective cell types (9,78), and, therefore, intracellular Ca^{2+} may be an important regulator of rab3-dependent pIgR trafficking. It shall be of significant interest in future studies to characterize the signaling pathway stimulated by dIgA binding to pIgR and to characterize the effect of dIgA on rab3D-pIgR interactions in lacrimal acinar cells.

The localization of pIgR to mature secretory granules in LGAC suggests that the pIgR has a motif that targets it to the regulated secretory pathway. Given the heterogeneity of the few motifs that have been characterized in proteins that are targeted to regulated secretory granules (31,37,60,70,74), scanning the pIgR sequence for such motifs has not yielded any useful information. Thus, the secretory granule targeting motif in the pIgR will need to be independently characterized. The assays used here to characterize the interaction of rab3D with pIgR may be valuable in characterizing this motif, and the lacrimal acinar cell system may be a good model system in which to pursue this line of investigation. In addition, the intracellular route taken by pIgR on its way to regulated secretory vesicles has yet to be characterized. Is the pIgR delivered to the regulated secretory pathway directly from the trans-Golgi network, similar to other tear proteins (76), or is there a novel route to the regulated secretory vesicles from the transcytotic pathway (Figure 10)? Since LGAC are not cultured in the presence of dIgA, dIgA would apparently not be necessary for the trafficking of the pIgR to secretory vesicles. What would be the purpose of a storage pool for pIgR in

NIH-PA Author Manuscript

NIH-PA Author Manuscript

NIH-PA Author Manuscript

secretory granules? Perhaps it is to secure a source for the generation of free SC in the presence of a relative abundance of dIgA. In addition to sIgA, free SC is highly abundant in the tear film, and most of the SC and sIgA in tears is produced by the lacrimal gland. It has been proposed that the free SC may play a significant role in mucosal immunity (46) by providing a scavenger function by binding to microorganisms in mucosal fluids (17,20), binding to interleukin-8 to regulate neutrophil function (34), or by regulating eosinophil function (39). All of these functions are certainly relevant to the secretion of SC into tears by lacrimal acinar cells to effect its protection of ocular surfaces.

In summary, we have reported a novel localization of the pIgR/SC to regulated secretory vesicles and a novel, functional interaction between rab3D and pIgR in a physiologically relevant system. We propose that rab3D regulates a novel pathway that results in the trafficking of the pIgR into the regulated secretory pathway, either directly from the trans-Golgi network or indirectly from the transcytotic pathway, or, conversely, that pIgR regulates the function of rab3D, as its putative GEF.

Acknowledgments

We would like to thank Francie Yarber for expert technical assistance.

GRANTS This work was supported by National Institutes of Health grants EY-11386 and EY-16985 (to S. Hamm-Alvarez). We acknowledge the Microscopy Subcore for the University of Southern California Center for Liver Diseases, supported by National Institutes of Diabetes and Digestive and Kidney Diseases (NIDDK) Core Center Grant P03 DK-48522.

ABBREVIATIONS

Ad	adenoviral
AE	apical endosomes
APM	apical plasma membrane
BE	basolateral endosomes
BLM	basolateral membrane
CCH	carbachol
dIgA	dimeric IgA
ER	endoplasmic reticulum
GEF	guanine nucleotide exchange factor
GFP	green fluorescent protein
GST	glutathione S-transferase
KO	knock-out
LGAC	lacrimal gland acinar cells
MDCK	Madin-Darby canine kidney
MOI	multiplicity of infection

NIH-PA Author Manuscript

NIH-PA Author Manuscript

NIH-PA Author Manuscript

Ni-NTA	Ni^{2+}- nitriloacetate
pIgR	polymeric immunoglobulin receptor
SC	secretory component
sIgA	secretory IgA
SV	secretory vesicle
TGN	trans-Golgi network
TRP	Transient Receptor Potential
WT	wild-type

REFERENCES

1. Allansmith MR, Radl J, Haaijman JJ, Mestecky J. Molecular forms of tear IgA and distribution of IgA subclasses in human lacrimal glands. J Allergy Clin Immunol. 1985; 76:569–576. [PubMed: 3932498]
2. An SJ, Hansen NJ, Hodel A, Jahn R, Edwardson JM. Analysis of the association of syncollin with the membrane of the pancreatic zymogen granule. J Biol Chem. 2000; 275:11306–11311. [PubMed: 10753942]
3. Apodaca G, Katz LA, Mostov KE. Receptor-mediated transcytosis of IgA in MDCK cells is via apical recycling endosomes. J Cell Biol. 1994; 125:67–86. [PubMed: 8138576]
4. Aroeti B, Kosen PA, Kuntz ID, Cohen FE, Mostov KE. Mutational and secondary structural analysis of the basolateral sorting signal of the polymeric immunoglobulin receptor. J Cell Biol. 1993; 123:1149–1160. [PubMed: 8245123]
5. Baldini G, Baldini G, Wang G, Weber M, Zweyer M, Bareggi R, Witkin JW, Martelli AM. Expression of Rab3D N135I inhibits regulated secretion of ACTH in AtT-20 cells. J Cell Biol. 1998; 140:305–313. [PubMed: 9442106]
6. Baldini G, Hohl T, Lin HY, Lodish HF. Cloning of a Rab3 isotype predominantly expressed in adipocytes. Proc Natl Acad Sci USA. 1992; 89:5049–5052. [PubMed: 1594612]
7. Barroso M, Sztul ES. Basolateral to apical transcytosis in polarized cells is indirect and involves BFA and trimeric G protein sensitive passage through the apical endosome. J Cell Biol. 1994; 124:83–100. [PubMed: 7905002]
8. Burstein ES, Brondyk WH, Macara IG. Amino acid residues in the ras-like GTPase Rab3A that specify sensitivity to factors that regulate GTP/GDP cycling of Rab3A. J Biol Chem. 1992; 267:22715–22718. [PubMed: 1331063]
9. Cardone MH, Smith BL, Mennitt PA, Mochly-Rosen D, Silver RB, Mostov KE. Signal transduction by the polymeric immunoglobulin receptor suggests a role in regulation of receptor transcytosis. J Cell Biol. 1996; 133:997–1005. [PubMed: 8655590]
10. Casanova JE, Wang X, Kumar R, Bhartur SG, Navarre J, Woodrum JE, Altschuler Y, Ray GS, Goldenring JR. Association of Rab25 and Rab11a with the apical recycling system of polarized Madin-Darby canine kidney cells. Mol Biol Cell. 1999; 10:47–61. [PubMed: 9880326]
11. Chen X, Edwards JA, Logsdon CD, Ernst SA, Williams JA. Dominant negative Rab3D inhibits amylase release from mouse pancreatic acini. J Biol Chem. 2002; 277:18002–19009. [PubMed: 11875077]
12. Chen X, Ernst SA, Williams JA. Dominant negative rab3D mutants reduce GTP-bound endogenous rab3D in pancreatic acini. J Biol Chem. 2003; 278:50053–50060. [PubMed: 14522985]
13. Childers NK, Bruce MG, McGhee JR. Molecular mechanisms of immunoglobulin A defense. Annu Rev Microbiol. 1989; 43:503–536. [PubMed: 2508540]

NIH-PA Author Manuscript

NIH-PA Author Manuscript

NIH-PA Author Manuscript

14. Corthesy B, Kraehenbuhl JP. Antibody-mediated protection of mucosal surfaces. Curr Top Microbiol Immunol. 1999; 236:93–111. [PubMed: 9893357]
15. da Costa SR, Yarber FA, Zhang L, Sonee M, Hamm-Alvarez SF. Microtubules facilitate the stimulated secretion of β-hexosaminidase in lacrimal acinar cells. J Cell Sci. 1998; 111:1267–1276. [PubMed: 9547304]
16. da Costa SR, Sou E, Yarber FA, Okamoto CT, Pidgeon M, Kessels MM, Mircheff AK, Schechter J, Qualmann B, Hamm-Alvarez SF. Impairing actin filament or syndapin functions promotes accumulation of clathrin-coated vesicles at the apical plasma membrane of polarized cells. Mol Biol Cell. 2003; 14:4397–4413. [PubMed: 12937279]
17. Dallas SD, Rolf RD. Binding of clostridium difficile toxin A to human milk secretory component. J Med Microbiol. 1998; 47:879–888. [PubMed: 9788811]
18. Darchen F, Goud B. Multiple aspects of Rab protein action in the secretory pathway: focus on Rab3 and Rab6. Biochimie. 2000; 82:375–384. [PubMed: 10865125]
19. Deneka M, Neeft M, van der Sluijs P. Regulation of membrane transport by rab GTPases. Crit Rev Biochem Mol Biol. 2003; 38:121–142. [PubMed: 12749696]
20. de Oliveira IR, de Araujo AN, Bao SN, Giugliano LG. Binding of lactoferrin and free secretory component to enterotoxigenic Escherichia coli. FEMS Microbiol Lett. 2001; 203:29–33. [PubMed: 11557136]
21. Gonzalez L Jr, Scheller RH. Regulation of membrane trafficking: structural insights from a Rab/effector complex. Cell. 1999; 96:755–758. [PubMed: 10102263]
22. Gudmundsson OG, Sullivan DA, Bloch KJ, Allansmith MR. The ocular secretory immune system of the rat. Exp Eye Res. 1985; 40:231–238. [PubMed: 3884354]
23. Hays LB, Wicksteed B, Wang Y, McCuaig JF, Philipson LH, Edwardson JM, Rhodes CJ. Intragranular targeting of syncollin, but not a syncollinGFP chimera, inhibits regulated insulin exocytosis in pancreatic beta-cells. J Endocrinol. 2005; 185:57–67. [PubMed: 15817827]
24. Hodel A, Edwardson JM. Targeting of the zymogen-granule membrane protein syncollin in AR42J and AtT-20 cells. Biochem J. 2000; 350:637–643. [PubMed: 10970774]
25. Hodges RR, Dartt DA. Regulatory pathways in lacrimal gland epithelium. Int Rev Cytol. 2003; 231:129–196. [PubMed: 14713005]
26. Hunziker W, Peters PJ. Rab17 localizes to recycling endosomes and regulates receptor-mediated transcytosis in epithelial cells. J Biol Chem. 1998; 273:15734–15741. [PubMed: 9624171]
27. Jerdeva GV, Wu K, Yarber FA, Rhodes CJ, Kalman D, Schechter JE, Hamm-Alvarez SF. Actin and non-muscle myosin II facilitate apical exocytosis of tear proteins in rabbit lacrimal acinar epithelial cells. J Cell Sci. 2005a; 118:4797–4812. [PubMed: 16219687]
28. Jerdeva GV, Yarber FA, Trousdale MD, Rhodes CJ, Okamoto CT, Dartt DA, Hamm-Alvarez SF. Dominant-negative PKC-epsilon impairs apical actin remodeling in parallel with inhibition of carbachol-stimulated secretion in rabbit lacrimal acini. Am J Physiol Cell Physiol. 2005b; 289:C1052–C1068. [PubMed: 15930141]
29. Jin M, Saucan L, Farquhar MG, Palade GE. Rab1a and multiple other Rab proteins are associated with the transcytotic pathway in rat liver. J Biol Chem. 1996; 271:30105–30113. [PubMed: 8939959]
30. Knop M, Aareskjold E, Bode G, Gerke V. Rab3D and annexin A2 play a role in regulated secretion of vWF, but not tPA, from endothelial cells. EMBO J. 2004; 23:2982–2992. [PubMed: 15257287]
31. Lacombe MJ, Mercure C, Dikeakos JD, Reudelhuber TL. Modulation of secretory granule-targeting efficiency by cis and trans compounding of sorting signals. J Biol Chem. 2005; 280:4803–4807. [PubMed: 15569678]
32. Larkin JM, Coleman H, Espinosa A, Levenson A, Park MS, Woo B, Zervoudakis A, Tinh V. Intracellular accumulation of pIgA-R and regulators of transcytotic trafficking in cholestatic rat hepatocytes. Hepatology. 2003; 38:1199–1209. [PubMed: 14578858]
33. Larkin JM, Woo B, Balan V, Marks DL, Oswald BJ, LaRusso NF, McNiven MA. Rab3D, a small GTP-binding protein implicated in regulated secretion, is associated with the transcytotic pathway in rat hepatocytes. Hepatology. 2000; 32:348–356. [PubMed: 10915742]

NIH-PA Author Manuscript

NIH-PA Author Manuscript

NIH-PA Author Manuscript

34. Marshall LJ, Perks B, Ferkol T, Shute JK. IL-8 released constitutively by primary bronchial epithelial cells in culture forms an inactive complex with secretory component. J Immunol. 2001; 167:2816–2823. [PubMed: 11509627]
35. Martelli AM, Baldini G, Tabellini G, Koticha D, Bareggi R, Baldini G. Rab3A and Rab3D control the total granule number and the fraction of granules docked at the plasma membrane in PC12 cells. Traffic. 2000; 1:976–986. [PubMed: 11208087]
36. Mestecky J, McGhee JR. Immunoglobulin A (IgA): molecular and cellular interactions involved in IgA biosynthesis and immune response. Adv Immunol. 1987; 40:153–245. [PubMed: 3296685]
37. Milgram SL, Mains RE, Eipper BA. Identification of routing determinants in the cytosolic domain of a secretory granule-associated integral membrane protein. J Biol Chem. 1996; 271:17526–17535. [PubMed: 8663411]
38. Mostov KE, Altschuler Y, Chapin SJ, Enrich C, Low SH, Luton F, Richman-Eisenstat J, Singer KL, Tang K, Weimbs T. Regulation of protein traffic in polarized epithelial cells: the polymeric immunoglobulin receptor model. Cold Spring Harb Symp Quant Biol. 1995; 60:775–781. [PubMed: 8824452]
39. Motegi Y, Kita H. Interaction with secretory component stimulates effector functions of human eosinophils but not of neutrophils. J Immunol. 1998; 161:4340–4346. [PubMed: 9780211]
40. Nguyen D, Jones A, Ojakian GK, Raffaniello RD. Rab3D redistribution and function in rat parotid acini. J Cell Physiol. 2003; 197:400–408. [PubMed: 14566969]
41. Ohnishi H, Ernst SA, Wys N, McNiven M, Williams JA. Rab3D localized to zymogen granules in rat pancreatic acini and other exocrine glands. Am J Physiol. 1996; 271:G531–G538. [PubMed: 8843780]
42. Ohnishi H, Samuelson LC, Yule DI, Ernst SA, Williams JA. Overexpression of Rab3D enhances regulated amylase secretion from pancreatic acini of transgenic mice. J Clin Invest. 1997; 100:3044–3052. [PubMed: 9399951]
43. Pavlos NJ, Xu J, Riedel D, Yeoh JS, Teitelbaum SL, Papadimitriou JM, Jahn R, Ross FP, Zheng MH. Rab3D regulates a novel vesicular trafficking pathway that is required for osteoclastic bone resorption. Mol Cell Biol. 2005; 25:5253–5269. [PubMed: 15923639]
44. Pellinen T, Arjonen A, Vuoriluoto K, Kallio K, Fransen JAM, Ivaska J. Small GTPase Rab21 regulates cell adhesion and controls endosomal traffic of β1-integrins. J. Cell Biol. 2006; 173:767–790. [PubMed: 16754960]
45. Pereira-Leal JB, Seabra MC. Evolution of the Rab family of small GTP-binding proteins. J Mol Biol. 2001; 313:889–901. [PubMed: 11697911]
46. Phalipon A, Corthesy B. Novel functions of the polymeric Ig receptor: well beyond transport of immunoglobulins. Trends Immunol. 2003; 24:55–58. [PubMed: 12547499]
47. Qian L, Wang Y, Xie J, Rose CM, Yang T, Nakamura T, Sandberg M, Zeng H, Schechter JE, Chow RH, Hamm-Alvarez SF, Mircheff AK. Biochemical changes contributing to functional quiescence in lacrimal gland acinar cells after chronic ex vivo exposure to a muscarinic agonist. Scand J Immunol. 2003; 58:550–565. [PubMed: 14629627]
48. Raffaniello RD, Lin J, Schwimmer R, Ojakian GK. Expression and localization of Rab3D in rat parotid gland. Biochim Biophys Acta. 1999; 1450:352–363. [PubMed: 10395946]
49. Raffaniello RD, Lin J, Wang F, Raufman JP. Expression of rab3D in dispersed chief cells from guinea pig stomach. Biochim Biophys Acta. 1996; 1311:111–116. [PubMed: 8630328]
50. Riedel D, Antonin W, Fernandez-Chacon R, de Toledo G Alvarez, Jo T, Geppert M, Valentijn JA, Valentijn K, Jamieson JD, Sudhof TC, Jahn R. Rab3D is not required for exocrine exocytosis but for maintenance of normally sized secretory granules. Mol Cell Biol. 2002; 22:6487–6497. [PubMed: 12192047]
51. Roa M, Paumet F, Le Mao J, David B, Blank U. Involvement of the ras-like GTPase rab3d in RBL-2H3 mast cell exocytosis following stimulation via high affinity IgE receptors (FcεRI). J. Immunol. 1997; 159:2815–2823. [PubMed: 9300704]
52. Rojas R, Apodaca G. Immunoglobulin transport across polarized epithelial cells. Nat Rev Molec Cell Biol. 2002; 3:944–956. [PubMed: 12461560]
53. Schimmoller F, Simon I, Pfeffer SR. Rab GTPases, directors of vesicle docking. J Biol Chem. 1998; 273:22161–22164. [PubMed: 9712825]

NIH-PA Author Manuscript

NIH-PA Author Manuscript

NIH-PA Author Manuscript

54. Schluter OM, Khvotchev M, Jahn R, Sudhof T. Localization versus function of Rab3 proteins. Evidence for a common regulatory role in controlling fusion. J Biol Chem. 2002; 277:40919–40929. [PubMed: 12167638]
55. Seachrist JL, Laporte SA, Dale LB, Babwah AV, Caron MG, Anborgh PH, Ferguson SS. Rab5 association with the angiotensin II type 1A receptor promotes Rab5 GTP binding and vesicular fusion. J Biol Chem. 2002; 277:679–685. [PubMed: 11682489]
56. Song W, Apodaca G, Mostov K. Transcytosis of the polymeric immunoglobulin receptor is regulated in multiple intracellular compartments. J Biol Chem. 1995; 267:29474–29480.
57. Sullivan DA, Allansmith MR. Hormonal influence on the secretory immune system of the eye: endocrine interactions in the control of IgA and secretory component levels in tears of rats. Immunology. 1987; 60:337–343. [PubMed: 3570355]
58. Sullivan DA, Bloch KJ, Allansmith MR. Hormonal influence on the secretory immune system of the eye: androgen control of secretory component production by the rat exorbital gland. Immunol. 1984; 52:234–246.
59. Tang LH, Gumkowski FD, Sengupta D, Modlin IM, Jamieson JD. Rab3D protein is a specific marker for zymogen granules in gastric chief cells of rats and rabbits. Gastroenterology. 1996; 110:809–820. [PubMed: 8608891]
60. Torii S, Saito N, Kawano A, Zhao S, Izumi T, Takeuchi T. Cytoplasmic transport signal is involved in phogrin targeting and localization to secretory granules. Traffic. 2005; 6:1213–1224. [PubMed: 16262730]
61. Tuvim MJ, Adachi R, Chocano JF, Moore RH, Lampert RM, Zera E, Romero E, Knoll BJ, Dickey BF. Rab3D, a small GTPase, is localized on mast cell secretory granules and translocates to the plasma membrane upon exocytosis. Am J Respir Cell Mol Biol. 1999; 20:79–89. [PubMed: 9870920]
62. Underdown BJ, Schiff JM. Immunoglobulin A: strategic defense initiative at the mucosal surface. Annu Rev Immunol. 1986; 4:389–417. [PubMed: 3518747]
63. Valentijn JA, Sengupta D, Gumkowski FD, Tang LH, Konieczko EM, Jamieson JD. Rab3D localized to secretory granules in rat pancreatic acinar cells. Eur J Cell Biol. 1996; 70:33–41. [PubMed: 8738417]
64. Valentijn JA, van Weeren L, Ultee A, Koster AJ. Novel localization of Rab3D in rat intestinal goblet cells and Brunner's gland acinar cells suggests a role in early Golgi trafficking. Am. J. Physiol. Gastrointest. Liver Physiol. 2007; 293:G165–G177. [PubMed: 17395899]
65. van de Graaf SFJ, Chang Q, Mensenkamp AR, Hoenderop JGJ, Bindels RJM. Direct interaction with rab11a targets the epithelial Ca^{2+} channels TRPV5 and TRPV6 to the plasma membrane. Mol Cell Biol. 2006; 26:303–312. [PubMed: 16354700]
66. van IJzendoorn SC, Tuvim MJ, Weimbs T, Dickey BF, Mostov KE. Direct interaction between Rab3b and the polymeric immunoglobulin receptor controls ligand-stimulated transcytosis in epithelial cells. Dev Cell. 2002; 2:219–228. [PubMed: 11832247]
67. van IJzendoorn SC, Mostov KE, Hoekstra D. Role of rab proteins in epithelial membrane traffic. Int Rev Cytol. 2003; 232:59–88. [PubMed: 14711116]
68. van Weeren L, de Graaff AM, Jamieson JD, Batenburg JJ, Valentijn JA. Rab3D and actin reveal distinct lamellar body subpopulations in alveolar epithelial type II cells. Am J Respir Cell Mol Biol. 2004; 30:288–295. [PubMed: 12933357]
69. Vetter IR, Wittinghofer A. The guanine nucleotide-binding switch in three dimensions. Science. 2001; 294:1299–1304. [PubMed: 11701921]
70. Waites CL, Mehta A, Tan PK, Thomas G, Edwards RH, Krantz DE. An acidic motif retains vesicular monoamine transporter 2 on large dense core vesicles. J Cell Biol. 2001; 152:1159–1168. [PubMed: 11257117]
71. Wang W, Sacher M, Ferro-Novick S. TRAPP stimulates guanine nucleotide exchange on Ypt1p. J Cell Biol. 2000; 151:289–295. [PubMed: 11038176]
72. Wang X, Kumar R, Navarre J, Casanova JE, Goldenring JR. Regulation of vesicle trafficking in MDCK cells by Rab11a and Rab25. J Biol Chem. 2000; 275:29138–29146. [PubMed: 10869360]
73. Wang Y, Jerdeva G, Yarber FA, da Costa SR, Xie J, Qian L, Rose CM, Mazurek C, Kasahara N, Mircheff AK, Hamm-Alvarez SF. Cytoplasmic dynein participates in apically targeted stimulated

NIH-PA Author Manuscript

NIH-PA Author Manuscript

NIH-PA Author Manuscript

secretory traffic in primary rabbit lacrimal acinar epithelial cells. J Cell Sci. 2003; 116:2051–2065. [PubMed: 12679381]

74. Wasmeier C, Burgos PV, Trudeau T, Davidson HW, Hutton JC. An extended tyrosine-targeting motif for endocytosis and recycling of the dense-core vesicle membrane protein phogrin. Traffic. 2005; 6:474–487. [PubMed: 15882444]
75. Weber E, Berta G, Tousson A, John PS, Green MV, Gopalokrishnan U, Jilling T, Sorscher EJ, Elton TS, Abramson DR, Kirk KL. Expression and polarized targeting of a Rab3 isoform in epithelial cells. J Cell Biol. 1994; 125:583–594. [PubMed: 8175882]
76. Wu K, Jerdeva GV, da Costa SR, Sou E, Schechter JE, Hamm-Alvarez SF. Molecular mechanisms of lacrimal acinar secretory vesicle exocytosis. Exp Eye Res. 2006; 83:84–96. [PubMed: 16530759]
77. Zerial M, McBride H. Rab proteins as membrane organizers. Nat Rev Mol Cell Biol. 2001; 2:107–117. [PubMed: 11252952]
78. Zoukhri D, Hodges RR, Sergheraert C, Dartt D. Cholinergic-induced Ca^{2+} elevation in rat lacrimal gland acini is negatively modulated by PKCδ and PKCε. Invest Ophthalmol Vis Sci. 2000; 41:386–392. [PubMed: 10670466]

NIH-PA Author Manuscript
NIH-PA Author Manuscript
NIH-PA Author Manuscript

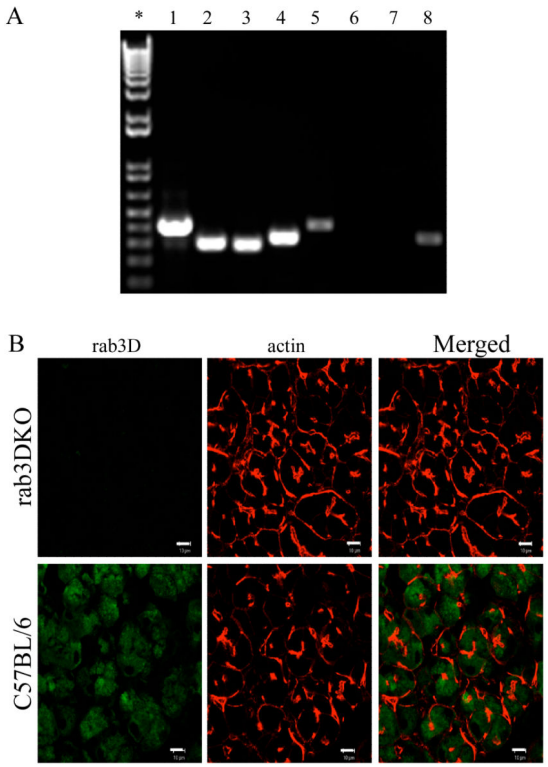

Figure 1.

RT-PCR of rab3 isoforms in mouse lacrimal gland and olfactory bulb and distribution of rab3D in lacrimal glands of rab3D KO and wild-type C57BL/6 mice. A. RT-PCR for rab3A, 3B, 3C, and 3D from mouse olfactory bulb (lanes 1, 2, 3, and 4, respectively) and mouse lacrimal gland (lanes 5, 6, 7, and 8 respectively). Rab3A and 3D are expressed in mouse lacrimal gland as shown in lanes 5 and 8, respectively. All four isoforms are expressed in olfactory bulb but only rab3a and 3D are expressed in lacrimal gland. The asterisk represents 1 Kb Plus DNA ladder. B. Lacrimal glands of rab3D KO and C57BL/6 mice were fixed, permeabilized, and stained with rabbit anti-rab3D polyclonal primary antibody and FITC-conjugated goat anti-rabbit secondary antibodies. F-actin was stained with rhodamine phalloidin. Immunofluorescence was observed with confocal microscopy. The lacrimal glands from rab3D KO mice showed no obvious alterations in actin cytoskeleton (red), but an absence of rab3D staining (green), compared to C57BL/c mice. Bar, 10 μm.

NIH-PA Author Manuscript

NIH-PA Author Manuscript

NIH-PA Author Manuscript

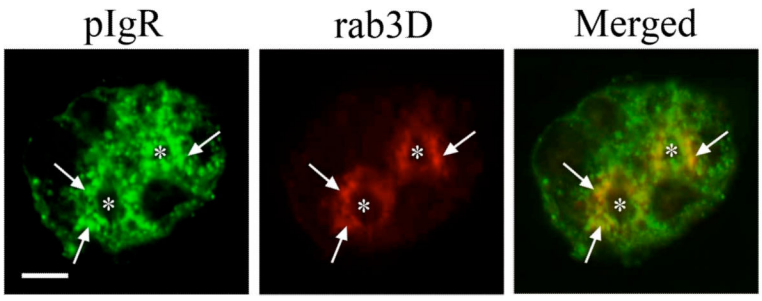

Figure 2.

Colocalization of rab3D and pIgR/SC in lacrimal gland acini reconstituted in primary culture. LGAC grown on Matrigel-coated coverslips were fixed, permeabilized and stained with primary sheep anti-SC and rabbit anti-rab3D antibodies, and secondary FITC-conjugated donkey anti-sheep and Alexa Fluor-568-conjugated goat anti-rabbit antibodies, respectively. Immunofluorescence was observed by confocal microscopy to localize rab3D and pIgR/SC in LGAC. Reconstituted acini are shown, comprised of approximately eight acinar cells surrounding two centrally located lumena (denoted by asterisks). Green, pIgR/SC; red, rab3D; arrows, regions of colocalization. Bar, 5μm. Results shown are representative of six independent experiments.

NIH-PA Author Manuscript
NIH-PA Author Manuscript
NIH-PA Author Manuscript

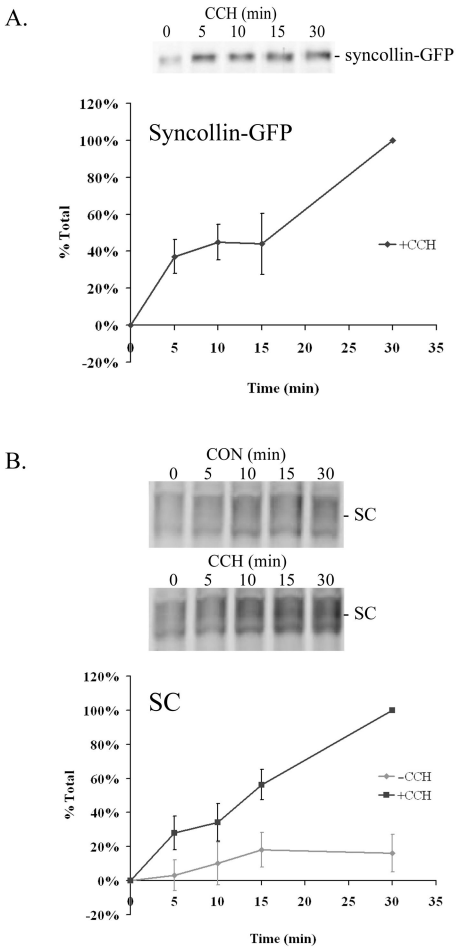

Figure 3.

SC released into the culture medium after carbachol stimulation is similar to the release of syncollin-GFP, a marker for the contents of a mature secretory vesicle. A. Western blots showing release of syncollin-GFP into culture medium in presence of 100 μM CCH for 0, 5, 10, 15, and 30 min in lacrimal gland acini transduced with Ad-syncollin-GFP. Rabbit anti-GFP antibody combined with a goat anti-rabbit IRDye800-conjugated secondary antibody was used to detect syncollin-GFP. Signals for syncollin-GFP (~40 kDa) were quantified and background intensity values subtracted. The quantitated intensity values were then normalized to pellet protein. Percent total was calculated by subtracting the baseline secretion of syncollin-GFP (t = 0 min) from each value, and then all values were compared to syncollin-GFP released after 30 min of CCH stimulation. Results are representative of six independent experiments. B. Western blots showing release of SC into culture medium in the presence of 100 μM CCH for 0, 5, 10, 15, and 30 min from reconstituted lacrimal gland acini. Sheep anti-SC antibody combined with a donkey anti-sheep IRDye700-conjugated secondary antibody was used to detect SC. Signals for SC (~70 kDa) were quantitated and background intensity values were subtracted. The quantitated intensity values were then normalized to total protein. Percent total was calculated in the same manner as for syncollin-GFP. The results shown are representative of six independent experiments.

NIH-PA Author Manuscript
NIH-PA Author Manuscript
NIH-PA Author Manuscript

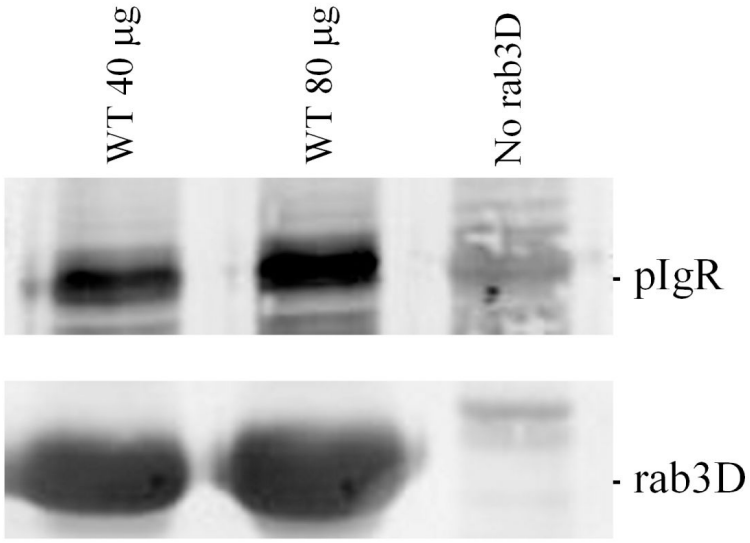

Figure 4.

Recombinant rab3DWT pull-down of pIgR. Rab3DWT expressed as $(His)_6$-tagged proteins in E. coli were purified on Ni-NTA bead columns, and 40 μg or 80 μg of rab3DWT was used in pull-down assays with lysates from resting LGAC. After rab3D was recovered from lysates by incubation with Ni-NTA beads, rab3D and any interacting proteins were eluted from the beads with SDS-PAGE buffer and analyzed by Western blot using primary anti-SC and anti-rab3D antibodies, and donkey anti-sheep IRDye700- and goat anti-rabbit IRDye 800- conjugated secondary antibodies, respectively. Results shown are representative of four independent experiments.

NIH-PA Author Manuscript
NIH-PA Author Manuscript
NIH-PA Author Manuscript

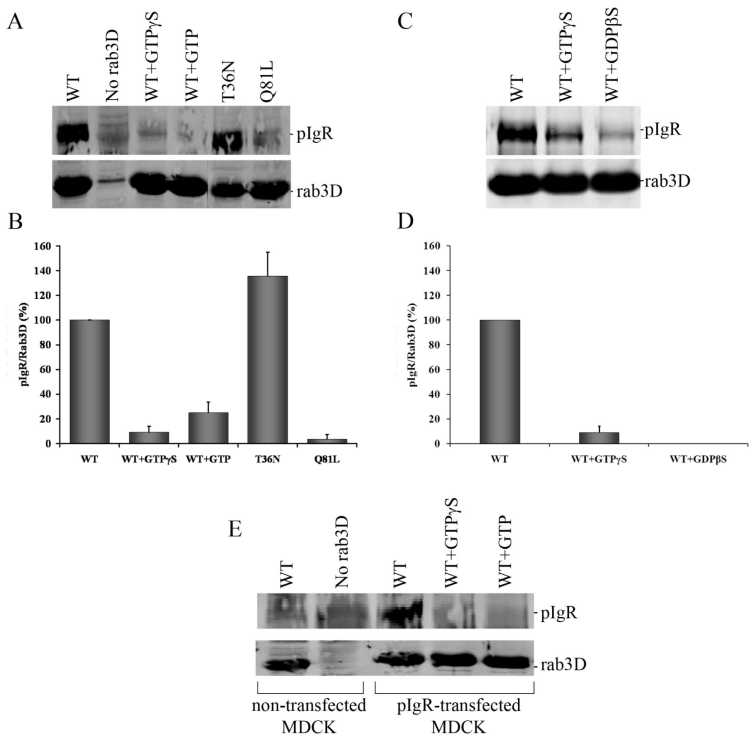

Figure 5.

Effect of mutations and nucleotides on recombinant rab3D pull-down of pIgR. A. Rab3DWT, constitutively active rab3DQ81L, and dominant-negative rab3DT36N expressed as $(His)_6$-tagged proteins in E. coli were purified, and 40 μg of each were used in pull-down assays with lysates from resting LGAC. In some cases, the lysate was supplemented with 10 μM GTPγS or 0.5 mM GTP. The binding of pIgR to rab3D was visualized by Western blot. B. Quantitation of the Western blots. Data are plotted as a ratio of pIgR binding to rab3D, with the ratio of pIgR binding to rab3DWT representing the 100% value (±S.E.M., n=3-9). C. Effect of GDPβS on binding of pIgR to recombinant $(His)_6$-tagged rab3DWT protein in pull-down assays. Lysates from resting LGAC were supplemented with 10 μM GTPγS (as a control) or 10 μM GDPβS. The binding of pIgR to rab3D was visualized by Western blot. D. Quantitation of Western blots was performed as in panel B (±S.E.M., n=4). E. Lysates from untransfected MDCK or pIgR-transfected MDCK cells were incubated with recombinant $(His)_6$-tagged rab3DWT in pull-down assays. In some cases, the lysate from pIgR-transfected MDCK cells was supplemented with 10 μM GTPγS or 0.5 mM GTP. The binding of pIgR to rab3D was visualized by Western blot. Results shown are representative of three independent experiments.

NIH-PA Author Manuscript

NIH-PA Author Manuscript

NIH-PA Author Manuscript

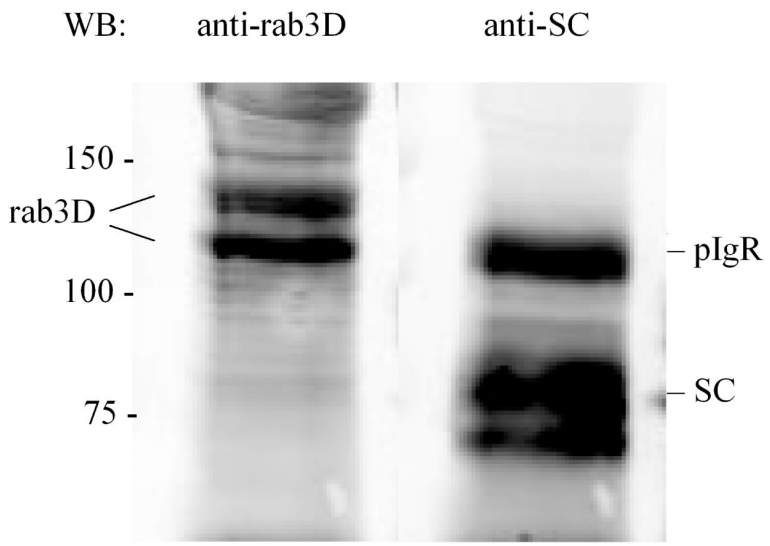

Figure 6.

Direct interaction between rab3D and pIgR on blot overlay. The pIgR was immunoprecipitated from LGAC with anti-SC antibody, resolved by SDS-PAGE, and transferred to nitrocellulose. The membrane was incubated with recombinant rab3DWT and subsequently probed with anti-rab3D antibodies. The immunoreactivity on the left lane shows the position of rab3D bound to the blot. The membrane was then stripped and re-probed with anti-SC antibody. The positions of immunoreactive bands for pIgR and SC are indicated on the right. The pIgR-reactive signal co-migrated precisely with the lower Mr protein of two rab3D-binding proteins, and rab3D did not bind to SC. Results shown are representative of three independent experiments.

NIH-PA Author Manuscript

NIH-PA Author Manuscript

NIH-PA Author Manuscript

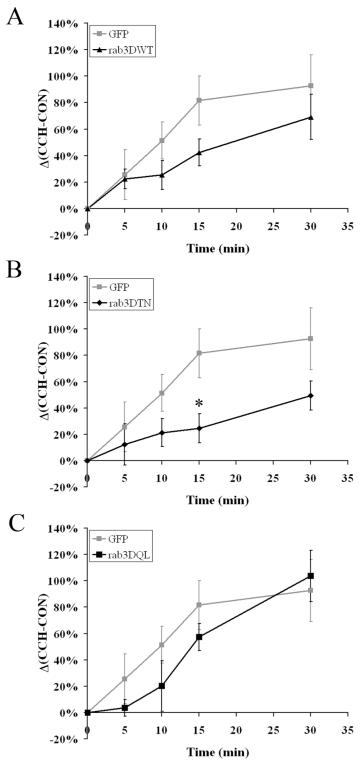

Figure 7.

Effect of adenovirus-mediated overexpression of rab3DWT and rab3D mutants on CCH-stimulated SC release in LGAC. A. Western blots of SC released into culture medium in the presence or absence of 100 μM CCH for 0, 5, 10, 15, and 30 min from LGAC, transduced with either Ad-GFP or Ad-rab3DWT were quantitated. Quantitated intensities were normalized to total protein. Percent of total secretion was calculated first by subtracting baseline secretion of SC (at t = 0 min) from each value for each time point and compared to SC released by 30 min CCH-stimulation of Ad-GFP-transduced cells. For each time point for each set of transduced acini, values from unstimulated glands were then subtracted from values from CCH-stimulated glands and graphed as Δ(CCH-CON). B. Comparison of SC released into culture medium in LGAC transduced with either Ad-GFP or dominant-negative Ad-rab3DT36N. SC release was analyzed as mentioned above. C. Comparison of SC release into culture medium in LGAC transduced with Ad-GFP or constitutively active Ad-rab3DQ81L. SC release was analyzed as mentioned above. Results are from six to eight independent experiments ±S.E.M. *Significant at $p \leq 0.05$.

NIH-PA Author Manuscript
NIH-PA Author Manuscript
NIH-PA Author Manuscript

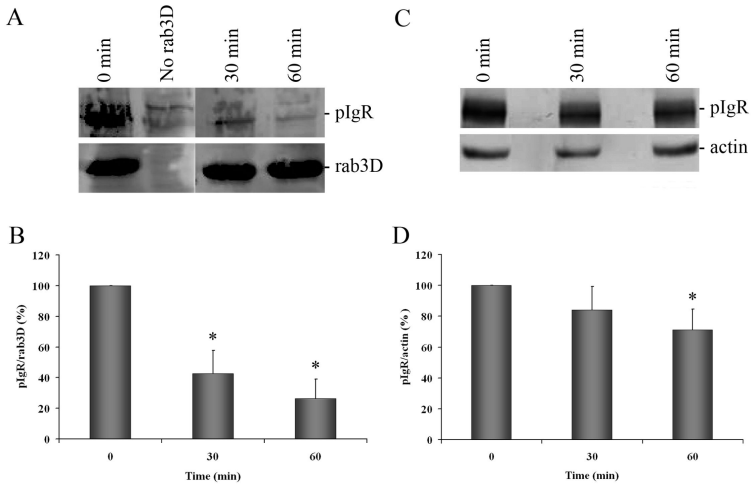

Figure 8.

Effect of CCH on rab3D-pIgR interaction and content of pIgR in CCH-stimulated lysate from LGAC. A. Rab3D-pIgR interaction in CCH-stimulated glands. Lysates from unstimulated (0 min) or 100 μM CCH-stimulated (30 or 60 min) LGAC were incubated with recombinant rab3DWT in pull-down assays. Binding of pIgR to rab3D was visualized by Western blot. B. The ratio of pIgR to rab3D was determined and normalized to that from resting LGAC (% of binding relative to that at 0 min). Results shown are from five independent experiments ±S.E.M. C. Content of pIgR in CCH-stimulated glands. Lysates from unstimulated (0 min) or 100 μM CCH-stimulated (30 or 60 min) LGAC were prepared, resolved by SDS-PAGE and transferred to nitrocellulose. Expression of pIgR and actin was visualized by Western blot analysis. D. The ratio of pIgR to actin was calculated and normalized to that from resting LGAC (% relative to that at 0 min). Results are from three independent experiments ±S.E.M. *Significant at $p \leq 0.05$.

NIH-PA Author Manuscript

NIH-PA Author Manuscript

NIH-PA Author Manuscript

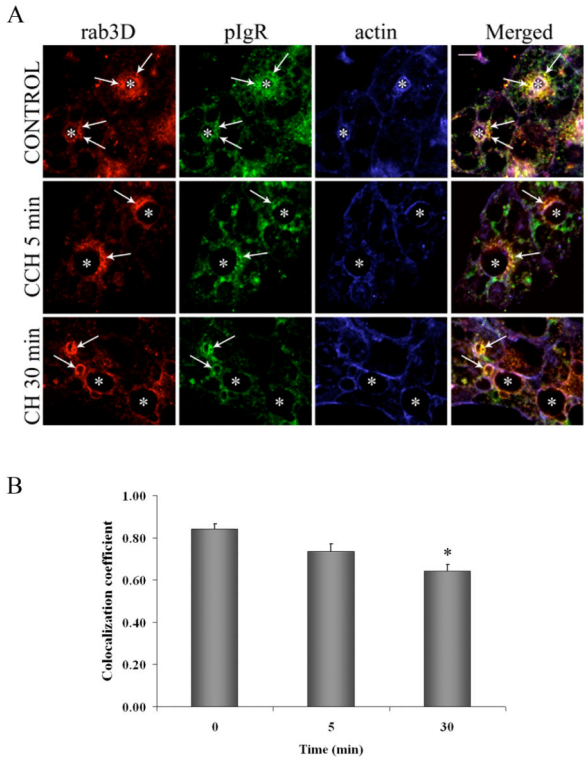

Figure 9.

Colocalization of SC/pIgR and rab3D in CCH-stimulated acini. A. Confocal micrographs of unstimulated control and 100 μM CCH-stimulated (5 and 30 min) LGAC. Rab3D (red), SC/pIgR (green), and actin (blue) are displayed as separate signals and as merged images. Arrows indicate areas of high colocalization between rab3D and SC/pIgR. Asterisks mark the lumena of the acini. Bar, 5 μm. B. Colocalization between rab3D and SC/pIgR around the subapical region (<2 μm beneath the lumen) was calculated. Values graphed are colocalization coefficients for SC/pIgR and reflect the relative numbers of colocalizing pixels, compared with the overall sum of pixel intensities above threshold and in that channel. The values range from 0 to 1, in which 0 indicates no colocalization, and 1 indicates that all pixels colocalize. Results were obtained from 41 (control, 0 min), 39 (CCH, 5 min), and 31 (CCH, 30 min) lumena imaged randomly over n = 3 separate preparations (6-15 lumena/preparaton). *Significant at $p \leq 0.05$.

NIH-PA Author Manuscript
NIH-PA Author Manuscript
NIH-PA Author Manuscript

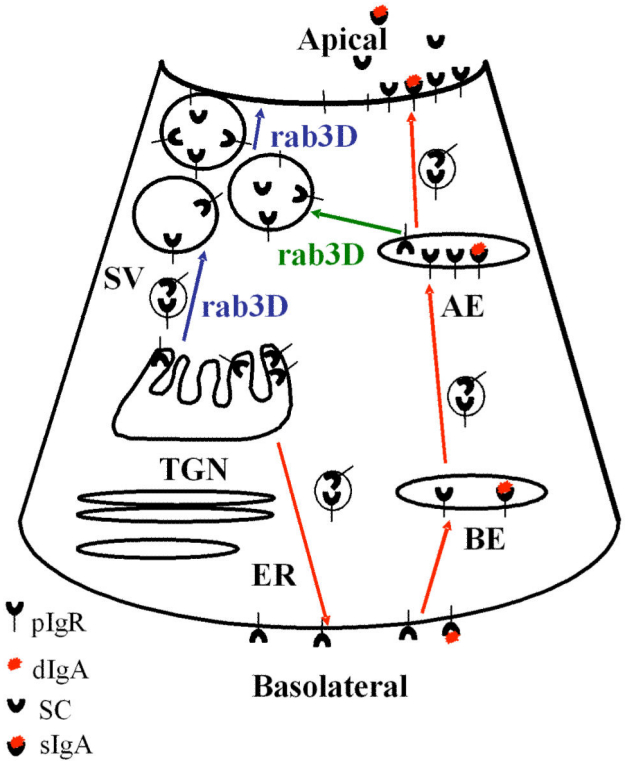

Figure 10.

Possible roles of rab3D in the regulation of pIgR trafficking and SC secretion in LGAC through the regulated mecrocrine and constitutive transcytotic pathways. After synthesis of pIgR in the endoplasmic reticulum (ER) and exit from trans-Golgi network (TGN), the pIgR is segregated into two groups in the TGN, one is sorted to regulated secretory vesicles (SV) by rab3D for the merocrine pathway (blue arrows), while the other is packaged into vesicles destined for the basolateral membrane for the transcytotic pathway (red arrows). An alternative route to regulated secretory vesicles may occur after the pIgR is first targeted to the transcytotic pathway (red arrows) (i.e., delivered to the basolateral cell surface followed by endocytosis and transported through a series of endosomal compartments), with some pIgR being recruited from apical endosomes (AE) to regulated vesicles by rab3D (green arrows) while the remainder continue along the constitutive transcytotic pathway (red arrows). BE, basolateral endosomes.